

C343e1

G-47

СООБЩЕНИЯ  
ОБЪЕДИНЕННОГО  
ИНСТИТУТА  
ЯДЕРНЫХ  
ИССЛЕДОВАНИЙ

ДУБНА



E7 - 7214

4430/2-73

**P.Gippner, K.-H.Kaun, W.Neubert, F.Stary,  
W.Schulze**

**EXCITATION OF KX-RAYS  
BY BOMBARDMENT OF THICK SOLID  
TARGETS WITH 150 MEV Xe IONS**

**1973**

**ЛАБОРАТОРИЯ ЯДЕРНЫХ РЕАКЦИЙ**

**E7 - 7214**

**P.Gippner, K.-H.Kaun, W.Neubert, F.Stary,  
W.Schulze**

**EXCITATION OF KX-RAYS  
BY BOMBARDMENT OF THICK SOLID  
TARGETS WITH 150 MEV Xe IONS**

## 1. Introduction

The investigation of characteristic  $X$ -rays, excited by the interaction of heavy ions with matter, shows that even the  $K$ -shells of the colliding partners become ionized with high probability. The order of magnitude of the cross section values  $\sigma_K$  as well as its dependence on the ion energy, on the atomic numbers of the projectile ( $Z_1$ ) and of the target ( $Z_2$ ) raise the question about the mechanism of the  $K$ -shell ionization. For ions with the smallest atomic numbers  $Z_1$ , such as protons and  $\alpha$ -particles, the experimentally determined values of the total cross section  $\sigma_K$  are in good agreement with that for direct Coulomb ionization<sup>[1-6]</sup>. For ion-target combinations, for which the relation  $Z_1 \ll Z_2$  is not valid, the measured cross sections  $\sigma_K$  exceed by several orders of magnitude the values predicted for Coulomb ionization<sup>[2]</sup>. In these cases the dependence of the cross sections  $\sigma_K$  and  $\sigma_L$  on the experimental parameters is described in a qualitative way by the molecular orbital (MO) model<sup>[2,7-12]</sup>. Unfortunately, no quantitative calculations of the cross sections, which are to be expected from the MO model, are so far carried out, so that direct experimental tests are currently impossible.

Some recent papers indicate that multiple collisions of ions in a target material lead to an asymmetric charge distribution, which contains also very high charge states<sup>[13,14]</sup>. Such high charge states may mainly result from outer shell ionization, but  $K$ -shell vacancies are not to be excluded. The concepts advanced so far on the formation of charge distributions by the interaction of ions

in solids, give no statements on the mechanism of an individual collision. The  $K$ -shell vacancies, necessary for the production of  $KX$ -rays may, therefore, originate from electron promotions as well as from any kind of direct process.

The investigations of  $K$  excitation cross sections, which are described in this paper, may contribute to clarify the mechanism of inner shell ionization in the case of high energies and heavy colliding ions.

## 2. Experimental Method

At the U-300 heavy ion cyclotron investigations of the emission of  $KX$ -radiation arising from the bombardment of different solid targets by  $^{136}\text{Xe}^{9+}$  ions were carried out. The ion energy was 150 MeV. Currents of about  $2 \times 10^{10}$  ions per second were used. The principal experimental arrangement was described earlier<sup>/15/</sup>. By means of a somewhat better focusing system, a focus of 6 mm in diameter was achieved at the target location. The targets consisted of thick metallic foils, covered by a frame of pure aluminium with an opening of  $15 \times 15 \text{ mm}^2$ . The parameters of the targets used are listed in table 1. Figure 1 shows the target-detector arrangement. The targets were exposed at an angle of  $45^\circ$  with respect to the beam direction, but the  $X$ -rays were measured perpendicularly to the beam direction. The grid of 0.1 mm tungsten wires, placed in front of the target, served to normalize the measured spectra to the equal quantities of incident ions.

For the detection of the  $KX$ -rays, a planar  $\text{Ge}(\text{Li})$  detector of about 11 mm thickness and 2.8 keV energy resolution at 60 keV energy was used\*. The measure-

---

\* The results of measurements with a  $\text{Si}(\text{Li})$  detector of 440 eV energy resolution at 26 keV full energy are in preparation.

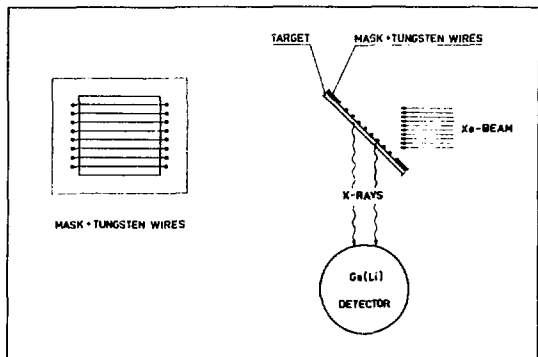


Fig. 1. Arrangement of target and detector.

ments were performed with a 1024-channel analyser. Figure 2 shows the energy spectrum obtained by bombardment of a *Bi* target.

No  $X$ -rays of energies below 10 keV could be detected due to an electrically inactive layer inside the detector. Therefore the  $LX$ -radiation of the target materials could not systematically be investigated. As a result of the Coulomb excitation of the lowest excited states of the tungsten nucleides  $^{182}\text{W}$ ,  $^{184}\text{W}$  and  $^{186}\text{W}$ , strong  $\gamma$ -ray transitions at 100.1 keV, 111.2 keV and 122.6 keV were obtained together with the characteristic  $KX$ -radiation of the collision partners (fig. 2). By means of the intensity of the Coulomb-excited  $\gamma$ -ray transitions, the normalization of the  $X$ -ray spectra to equal charges was carried out.

In order to obtain the absolute cross section values, the charge was measured without target foil. The number of Coulomb-excited  $\gamma$ -rays of the tungsten grid was compared with the charge of the ions getting through the grid to the Faraday cup. In this way any falsification

Table 1

The types of targets used. The symbols designate the following:  $Z_1$  and  $Z_2$ , the atomic numbers of projectile and target, respectively;  $d'$ , the effective target thickness;  $R_0$ , the range of 150 MeV  $Xe^{123+}$  ions.

Target	$Z_2$	$Z_1/Z_2$	$\frac{\rho}{g/cm^3}$	$\frac{d'}{mg/cm^2}$	$\frac{R_0}{mg/cm^2}$
Rh	45	1.20	12.4	19.4	6.4
Ag	47	1.15	10.5	11.7	8.6
La	57	0.95	6.15	20.0	9.7
Gd	64	0.84	7.95	6.2	11.9
Lu	71	0.76	9.74	6.2	13.1
Au	79	0.68	19.3	20.9	14.2
Bi	83	0.65	9.7	139.6	14.6

of the charge measurement due to changes in the charge of the  $Xe$  ions inside the target was avoided.

The following corrections are to be made in the target arrangement in fig. 1.

1. Self-absorption of the  $X$ -rays within the range of the  $Xe$  ions in the target as well as absorption in penetrating the target dead layers\*.
2. Absorption of the tungsten grid  $\gamma$ -radiation by the target. The whole target thickness is effective for this purpose.
3. Excitation of Xenon  $KX$ -radiation by the tungsten grid. Its portion was determined by a measurement without target, which was also normalized to the intensity of the Coulomb-excited  $\gamma$ -ray transitions of the tungsten grid.
4. In the case of the  $Gd$  and  $Lu$  targets, Coulomb-excited  $\gamma$ -ray transitions were obtained, the inner conversion of which contributes to the target  $KX$ -ray intensity. Its portion was calculated from the intensity of the respective  $\gamma$ -ray lines and the known conversion coefficients.

The rate of  $KX$ -radiation, measured with our target-detector arrangement, is given by the following relation:

$$N_m = \int n \sigma [E(r)] e^{-\mu(d'-r)} dr, \quad (1)$$

where  $E(r)$  is an ion energy dependent on the penetration depth along a stretched path inside the target;  $\sigma[E(r)]$  is the cross section as a function of the ion energy. The value

---

\* In ref. <sup>16/</sup> it was supposed that the  $K_{\alpha}$ -radiation of  $Ce$  ions was emitted only in a thin target layer of about  $100 \mu g/cm^2$ . The account of this effect would considerably alter our absorption correction, and enlarge the cross section values  $\sigma_K^{\alpha}(Xe)$  by more than one order of magnitude. Since this effect has not been explained, we assume that the target radiation as well as the  $Xe$ -radiation was homogeneously excited over the entire range of  $Xe$  ions.

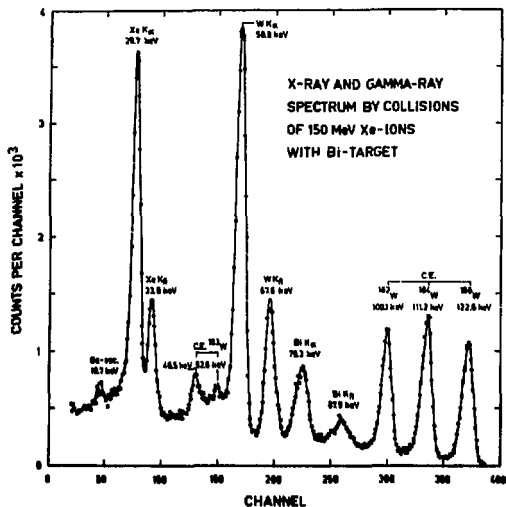


Fig. 2. The spectrum obtained by Xe ion bombardment of a bismuth target together with a tungsten grid.

of  $\bar{\sigma} = \sigma(E)$  averaged over the range  $R_0$  of the Xe ions and dependent only on incident energy  $E$ , is obtained from eq. (1) by making use of some correction factors

$$\bar{\sigma} = \sigma(E) = \frac{\mu N_{mc}}{n \epsilon_{tot} MD e^{-\mu(d'-R_0)} (1 - e^{-\mu R_0})}, \text{ for } R_0 < d'$$

or

$$\bar{\sigma} = \sigma(E) = \frac{\mu N_{mc}}{n \epsilon_{tot} MD (1 - e^{-\mu d'})}, \text{ for } R_0 > d', \quad (2)$$



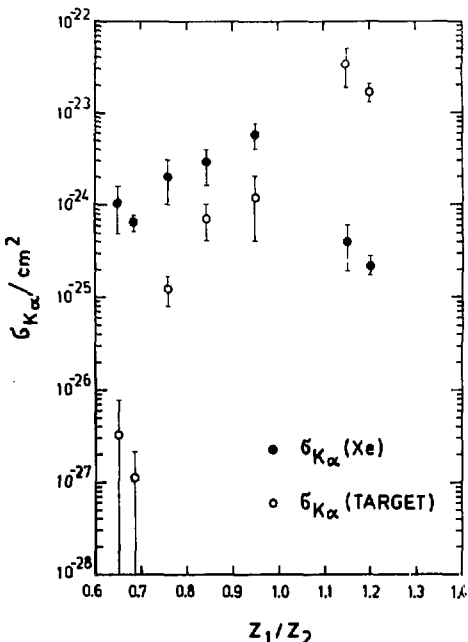


Fig. 3. Absolute cross sections  $\sigma_{K\alpha}(\text{Xe})$  and  $\sigma_{K\alpha}(\text{target})$  as a function of the ratio of the atomic numbers of projectile ( $Z_1$ ) and target ( $Z_2$ ). The abscissa allows to compare the obtained results with those of ref.<sup>12/</sup> which, in spite of the preferential use of Ne ions, shows in principle the similar dependence of  $\sigma_K$  on  $Z_1/Z_2$ .

where  $N_{mc}$  is the measured and corrected number of  $K_{\alpha}X$ -ray quanta. In calculating the cross section  $\sigma_{K\alpha}(\text{Xe})$ , the Xe  $K_{\alpha}$ -radiation excited by the tungsten grid was subtracted. In calculating the cross sections  $\sigma_{K\alpha}(\text{target})$  for Gd and Lu, the inner conversion of the

Coulomb-excited  $\gamma$ -ray transitions was taken into account;

$\mu$  is the target absorption coefficient for the  $K_{\alpha}$ -radiation;

$d'$  is the effective thickness of the target material;

$n$  is the number of target atoms per  $\text{cm}^3$ ;

$\epsilon_{tot}$  is the total efficiency of the  $\text{Ge(Li)}$  detector;

$D$  is the number of Coulomb-excited  $\gamma$ -rays of the tungsten grid, acting as a normalization factor;

$M$  is a calibration factor obtained from the absolute charge measurement for  $\text{Xe}^{2+}$  ions.

### 3. Experimental Results

In table 2, the measured cross section values  $\sigma_{K_{\alpha}}$  for  $\text{Xe}$  and the investigated targets as well as the ratios  $\sigma_{K_{\alpha}}(\text{target})/\sigma_{K_{\alpha}}(\text{Xe})$  are summarized. Figure 3 shows the dependence of these cross sections on the ratio of the atomic numbers  $Z_1/Z_2$  for a constant incident energy of 150 MeV. In the calculations of the errors  $\Delta\sigma_{K_{\alpha}}$ , given in table 2 and fig. 3, only the errors in the peak areas  $N_{\text{pic}}$  and  $D$ , the target thicknesses  $d'$ , the absorption coefficients  $\mu$  and the ranges  $R_0$  have been taken into account. These values are uncertain from target to target and affect the relative positions of several points in fig. 3. The neglected errors of the detector efficiency  $\epsilon_{tot}$  and the calibration factor  $M$  influence to an equal extent all the points of fig. 3, i.e., only the absolute cross section values. The account of the systematical errors  $\Delta\epsilon_{tot}$  and  $\Delta M$  increases the relative errors  $\Delta\sigma_{K_{\alpha}}/\sigma_{K_{\alpha}}$  by 25%.

The dependence of the cross section  $\sigma_{K_{\alpha}}$  on  $Z_1/Z_2$  is characterized by the following:

1. the cross section  $\sigma_{K_{\alpha}}(\text{target})$  decreases with growing atomic number  $Z_2$ , whereas  $\sigma_{K_{\alpha}}(\text{Xe})$  shows a resonancelike behaviour with a maximum at  $Z_2 = Z_1$ .
2. the cross section ratio  $\sigma_{K_{\alpha}}(\text{target})/\sigma_{K_{\alpha}}(\text{Xe})$  shows that the  $K$ -shell of the colliding partner having the smaller atomic number is preferably ionized.

#### 4. Discussion

The experimental facts, described in section 3, may be explained qualitatively by means of the molecular orbital (MO) model <sup>/9,11/</sup>. This model handles the limiting case of an adiabatic collision, in which the relative velocity  $v$  of the colliding partners is small compared to the velocity  $u$  of the atomic shell electrons. The approach of both atoms causes a strong perturbation in the Coulomb potential and consequently in the electron motion. Under the condition  $v \ll u$ , the electron configuration is able to follow the perturbation. For final distances  $R$  between the colliding particles a "quasimolecule" with common electron shells is formed; but in the limiting case  $R \rightarrow 0$  we can speak of a "quasiatom \*". The energy eigenvalues of the wave functions of the quasimolecule may be given as a function of the distance  $R$ . In the frame of the MO model this dependence is discussed on the basis of the hydrogen molecule theory <sup>/17,18/</sup>. For  $R \rightarrow 0$  and  $R \rightarrow \infty$ , the atomic levels are characterized by the main quantum numbers  $n$  and the quantum numbers  $l$  of the orbital momentum. For small distances  $R$  the levels split into states, which are described by the additional quantum number  $\lambda$  representing the projection of the orbital momentum  $l$  on the axis of the molecule ( $0 \leq \lambda \leq l$ ). The notations  $\sigma, \pi, \delta, \phi$  are used for  $\lambda = 0, 1, 2, 3$ , respectively.

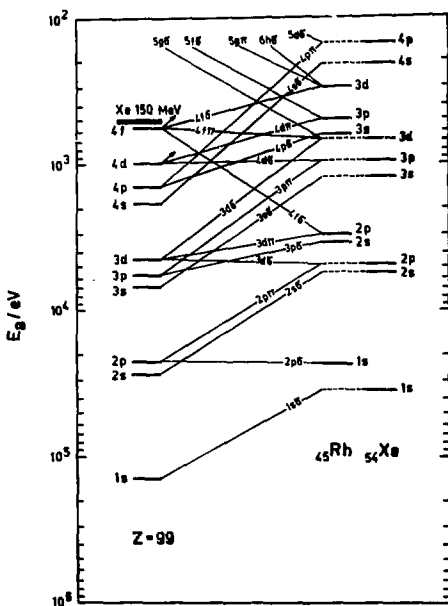
The spin-orbital coupling of the electrons has been neglected. By drawing the principal behaviour of the energy states  $E(nl\lambda)$  as a function of  $R$ , a correlation scheme is obtained, which provides information on the occupation of the quasimolecular states by the electrons of both atoms. In fig. 4 correlation schemes are drawn for the systems  $Rh+Xe$  and  $Gd+Xe$ . On the basis of the MO model,

---

\* Nuclear reactions may be neglected, because the ion energy used is far below the Coulomb barrier.

the origin of characteristic X-rays may be understood in the following way:

- a) the level splitting leads to changes in the main quantum numbers of electrons (promotion) and sometimes to drastic changes of the electron binding energies during the formation of a quasimolecule or a quasiautom;
- b) at the crossing points of molecular levels a certain probability exists for transitions of electrons from one state to another. Such a transition probability exists mainly for the asymptotic crossings  $R \rightarrow 0$  and  $R \rightarrow \infty$ , where the molecular levels join the atomic ones;



c) Vacancies are produced by electron transitions from an occupied to an unoccupied level. If the lifetime of a vacancy exceeds the collision time, it can be transferred to the other collision partner and give rise to its characteristic X - radiation.

In principle, the MO model is applicable to our experiment, because the condition  $v \ll u$  is fulfilled for every target and the principal quantum numbers  $n = 1, 2$  and 3. For the  $M$  -shell of  ${}_{45}Rh$  the condition  $v/u = 0.3$  is

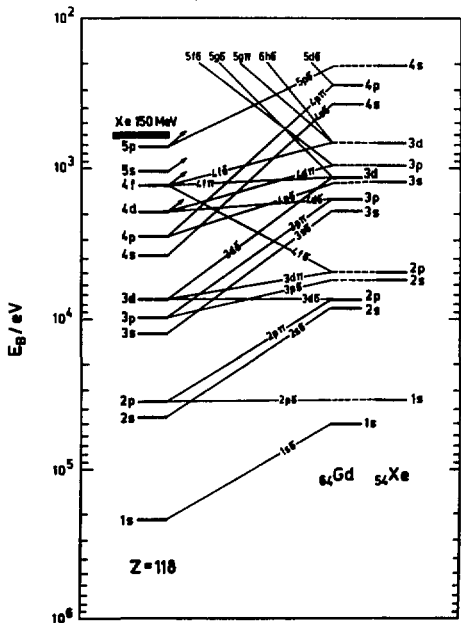


Fig. 4. MO correlation schemes for the asymmetric collision systems  $Rh + Xe$  (a) and  $Gd + Xe$  (b).

valid. This ratio decreases further with increasing  $Z$  of the target and decreasing quantum number  $n$ . The time required for penetration of the  $K$ - and  $L$ - shells of the collision partners is of the order of  $10^{-18}$  s, whereas for solid targets the time between two collisions amounts to about  $10^{-17}$  s. Vacancies in the  $M$ -,  $L$ - and  $K$ -shells of  $Xe$  have lifetimes of  $10^{-14}$ ,  $10^{-15}$  and  $10^{-16}$  s respectively<sup>/19/</sup>. They are, therefore, able to survive several collisions and to give rise to the emission of characteristic  $X$  -rays after the particles have been separated.

The microscopic processes, which lead to the formation of inner shell vacancies, may be described in the following way. Energetic ions entering a target undergo a further loss of shell electrons. On the other hand, they capture electrons from the target atoms. Already after the ions have penetrated a very thin target layer, a new equilibrium charge distribution is formed<sup>/14/</sup>, which allows to define a mean charge state  $\bar{q}$  of the ions. It may be expected that, after penetration of thick layers, the mean charge  $\bar{q}$  decreases again due to the energy loss of the ions. For solid targets,  $\bar{q}$  shows only a slight dependence on the target materials<sup>/14,20/</sup>. After penetration of gold foils by  $Xe^{8+}$  ions with an energy  $E_{lab} = 130$  MeV a mean value  $\bar{q} = 26$  has been found<sup>/21/</sup>. This value is satisfactorily reproduced by a formula given in ref.<sup>/20/</sup>, which for 130 MeV  $Xe$  ions gives  $\bar{q} = 26.9$  and for 150 MeV  $Xe$  ions gives  $\bar{q} = 28$ . It may, therefore, be assumed, that after some collisions with the outermost target layer a large number of  $Xe$  ions shows vacancies in the  $3d$ -shell. As is shown in fig 4a for a target with  $Z_2 < 54$ , according to the MO model, vacancies may get across the  $3d\delta$  -term to the  $3d$  -term of the quasiatom with  $Z = 99$  and therefrom into the  $2p$ -shell of the  $Xe$  ion. Filling these vacancies by outer electrons causes  $LX$  -rays of  $Xe$ . If, however, during the lifetime of the  $2p$  vacancy a further collision takes place, the vacancy may be transferred into the  $1s$  -shell of the  $Rh$  atom. Multiple collisions lead to the excitation of  $KX$  -radiation of  $Rh$ . If the atomic number  $Z_2$  nearly agrees with that of  $Xe$ , i.e., both target and projectile have almost equal  $K$  binding energies, also the  $1s$  -electrons of  $Xe$  may be promoted

Table 2  
 Cross sections  $\sigma_K$  for the excitation of  $K_\alpha X$  -rays by  
 bombardment with 150 MeV Xe ions

Target	$\sigma_{K_\alpha}(\text{target}) \pm \Delta\sigma_{K_\alpha}$ cm <sup>2</sup>	$\sigma_{K_\alpha}(\text{Xe}) \pm \Delta\sigma_{K_\alpha}$ cm <sup>2</sup>	$\sigma_{K_\alpha}(\text{target})$ $\sigma_{K_\alpha}(\text{Xe})$
Rh	$(1.7 \pm 0.4) \times 10^{-23}$	$(2.2 \pm 0.5) \times 10^{-25}$	$77.3 \pm 35.7$
Ag	$(3.4 \pm 1.6) \times 10^{-23}$	$(4.0 \pm 2.1) \times 10^{-25}$	$85.0 \pm 84.6$
La	$(1.2 \pm 0.8) \times 10^{-24}$	$(5.8 \pm 1.8) \times 10^{-24}$	$(2.1 \pm 2.1) \times 10^{-1}$
Gd	$(7.2 \pm 2.8) \times 10^{-25}$	$(2.8 \pm 1.2) \times 10^{-24}$	$(2.6 \pm 2.1) \times 10^{-1}$
Lu	$(1.2 \pm 0.4) \times 10^{-25}$	$(2.0 \pm 1.0) \times 10^{-24}$	$(6.0 \pm 5.0) \times 10^{-2}$
Au	$(1.1 \pm 1.0) \times 10^{-27}$	$(6.4 \pm 1.1) \times 10^{-25}$	$(1.7 \pm 1.8) \times 10^{-3}$
Bi	$(3.2 \pm 4.5) \times 10^{-27}$	$(1.0 \pm 0.5) \times 10^{-24}$	$(3.2 \pm 6.1) \times 10^{-3}$

into the higher states with high probability, resulting in a big cross section  $\sigma_K(Xe)$  (fig. 3). This mechanism explains qualitatively that for  $Z_2 < 54$  preferably the lighter collision partner becomes  $K$  ionized.

In fig. 4b the correlation scheme is drawn for the system  $Gd + Xe$ , which is in principle also valid for all other targets with  $Z_2 > 54$ . In spite of the increasing electron binding energies with increasing  $Z_2$ , the alternating shell sequence  $K_T - K_{Xe} - L_T - L_{Xe} - M_T - M_{Xe}$  is preserved up to the system  $Bi + Xe$ . According to the already described mechanism, vacancies of the  $3d$ -shell of  $Xe$  ions may be transferred during further collisions into the  $2p$ -shell of  $Xe$  and therefrom into the  $2p$ -shell of  $Gd$ . A strong  $L$  ionization of both partners is to be expected.

In order to explain the origin of  $KX$ -radiation of  $Xe$ , the following processes might be discussed:

- a) collisions of  $Xe$  ions with  $L$  ionized  $Gd$  atoms, and
- b) collisions of  $L$  ionized  $Xe$  ions with  $Xe$  atoms, implanted into the target lattice.

Similar arguments are used in paper <sup>/22/</sup> to explain the  $KX$ -radiation of  $Ne$  ions, originating from bombardment of an  $Ar$  gas target. For both types of collisions, only a very low rate determined by the ratio of the particle densities is to be expected. Neglecting the back diffusion of the ions, in the collisions of  $Xe$  with  $Xe$  an accumulation effect should be observed. At the end of a 30 min. irradiation, the ion current leads to one  $Xe + Xe$  collision, compared with  $10^5$   $Gd + Xe$  collisions. Experimentally no alteration of the intensity ratio of the target and Xenon radiation has been found with an accuracy of a few percent for an irradiation period of 1.5 hours.

The origin of the  $KX$ -radiation of  $Gd$  could be explained as being due to recoils of  $L$  ionized  $Gd$  target atoms. During the formation of quasimolecules with other target atoms,  $K$ -shell vacancies may be produced in the symmetric colliding system. In this way the formation of target  $KX$ -rays may in principle be understood also for targets with  $Z_2 > 54$ .

For the minimum distance between the colliding particles the relation



$$R_{min} = \frac{\epsilon^2 Z_1 Z_2}{E_{lab}} \cdot \frac{M_1 + M_2}{M_2} \quad (3)$$

is valid. Provided that the energy  $E_{lab}$  of the  $Xe$  ions is constant,  $R_{min}$  increases with increasing  $Z_2$ . In addition, with increasing  $Z = Z_1 + Z_2$  the crossings of the molecule terms are shifted  $\llcorner \llcorner$  in the direction of  $R \rightarrow 0$ . Both effects lead to a decrease in the following ionization cross sections:

- a)  $\sigma_L(Xe)$  for  $L$  ionization of the  $Xe$  ions in collisions with target atoms.
- b)  $\sigma_K(\text{target})$  for  $K$  ionization of recoiled target atoms in collisions with target atoms.

This leads to a decrease in  $\sigma_K(\text{target})$  with decreasing  $Z_1/Z_2$  (fig. 3).

### Summary

1. For the bombardment of several targets with 150 MeV  $Xe$  ions the absolute cross sections  $\sigma_K(Xe)$  and  $\sigma_K(\text{target})$  have been measured.

2. The discussion of the experimental results shows that for  $Z_2 < 54$  the MO model is able to explain the cross section ratios  $\sigma_{K_a}(\text{target})/\sigma_{K_a}(Xe)$  in a qualitative way. Moreover, from this model it may be expected that the cross section  $\sigma_{K_a}$  of the projectile shows a maximum in the case of a symmetric collision system  $Z_1 = Z_2$ . For  $Xe$  ions the height and position of this maximum may be interpolated from the measured cross section curve

$\sigma_{K_a}(Xe)$ .

3. For  $Z_2 > 54$ , the  $KX$ -radiation of  $Xe$  and the target materials are no longer understood on the basis of multiple collisions of  $Xe$  ions with target atoms. An explanation of the  $Xe$  radiation with the help of the collisions of  $Xe$  ions with implanted  $Xe$  atoms is improbable. For a possible explanation of the target radiation, use was made of target recoil collisions. The  $Z_2$  dependence of  $\sigma_K(Xe)$  and  $\sigma_K(\text{target})$  for  $Z_2 > 54$  gives a hint at the formation of quasimolecules in this case too.

The authors would like to thank Academician G.N.Flerov for his interest in the problem, Dr. V.A.Karnaikhov for stimulating discussions, the heavy-ion cyclotron staff for their cooperation and Mrs. I.Schulze for her technical help.

### References

1. E.Merzbacher and H.W.Lewis. Handbuch der Physik, ed. by E.Flügge, Springer-Verlag Berlin, 1958, Vol.34, p. 166.
2. W.Brandt and R.Laubert. Phys. Rev. Lett., 24, 1037 (1970).
3. J.M.Hansteen and O.P.Mosebakk. Z.Phys., 234, 281 (1970).
4. R.L.Watson, C.W.Lewis and J.B.Natowitz. Nucl. Phys., A 154, 561 (1970).
5. J.M.Hansteen and O.P.Mosebakk. Contr. to the Proceedings of the International Conf. on Inner Shell Ionization Phenomena, Atlanta 1972.
6. O.N.Jarvis and C.Whitehead. Phys. Rev., A5, 1198 (1972).
7. W.Lichten. Phys. Rev., 164, 131 (1965).
8. H.J.Specht. Z.Phys., 185 301 (1965).
9. U.Fano and W.Lichten. Phys. Rev. Lett., 14, 627 (1965).
10. J.Macek. Phys. Rev. Lett., 28, 1298 (1972).
11. M.Barat and W.Lichten. Phys. Rev., A 6, 211 (1972).
12. H.O.Lutz, J.Stein, S.Datz and C.D.Moak. Phys. Rev. Lett., 28, 6, (1972).
13. G.A.Ryding, A.B.Wittkower and P.H.Rose. Phys. Rev., A3, 1658 (1971).
14. H.D.Betz. Rev. Mod. Phys., 44, 465 (1972).
15. U.Hagemann, W.Neubert, W.Schulze and F.Stary. Nucl. Instr. Meth., 9C, 415 (1971).
16. H.W.Schnopper, A.R.Sohval, H.D.Betz, J.P.Delvaile, K.Kalata, K.W.Jones and H.E.Wegner. Contr. to the Proceedings of the International Conf. on Inner Shell Ionization Phenomena, Atlanta 1972.
17. P.H.Morse and E.C.G.Stückelberg. Phys. Rev., 33, 932 (1929).
18. H.Bethe. Handbuch der Physik, ed. by H.Geiger, Berlin 1933, Vol. XXIV, part I, p. 530.
19. H.R.Rosner and C.P.Bhalla. Z.Phys., 231, 347 (1970).
20. V.S.Nikolajew and I.S.Dmitriev. Phys. Lett., 28A, 277 (1968).
21. И.А.Шелев и др. ОИЯИ, П9-8062, Дубна, 1971.

22. H.Tawara and J.Kistemaker. Phys. Lett., 41A, 287 (1972).
23. L.C.Northcliff and R.F.Schilling. Nucl. Data Tables, A 7, 233 (1970).

Received by Publishing Department  
on June 1, 1973.